

TITANIUM ISOTOPE SYSTEMATICS OF REFRACTORY INCLUSIONS: ECHOES OF MOLECULAR CLOUD HETEROGENEITY. Q.R. Shollenberger¹, J. Render², M. K. Jordan³, K.A. McCain¹, S. Ebert⁴, A. Bischoff⁴, T. Kleine⁴, and E. D. Young¹, ¹Department of Earth, Planetary, and Space Sciences, University of California Los Angeles, Los Angeles, CA, USA (qshollenberger@ucla.edu), ²Lawrence Livermore National Laboratory, Livermore, CA, USA, ³Geophysical Laboratory, Carnegie Institution for Science, Washington, DC, USA, ⁴Institut für Planetologie, University of Münster, Münster, Germany

Introduction: Calcium-aluminum-rich inclusions (CAIs) are the oldest dated solids known to have formed within the Solar System. Their chemical and isotopic signatures provide a sampling of the earliest reservoirs present in the Solar System and how these reservoirs evolved and mingled through time. Previous work has shown that CAIs have mass-independent (nucleosynthetic) isotope anomalies compared to later formed Solar Systems solids [*e.g.*, 1-2]. However, thus far, the only confirmed carrier of isotopically anomalous material has been nanospinel that show large enrichments in ⁵⁴Cr [3-4].

In this study, we use two different methodologies to assess the carriers of the Ti isotope anomalies in CAIs. The first approach is examining 15 CAIs of variable sizes from CV3 chondrites with laser ablation multicollector inductively coupled plasma mass spectrometry (LA-MC-ICPMS) to probe different Ti-bearing CAI mineral phases. For these data, Type A CAIs, especially fluffy Type A, are of particular interest as these objects are believed to have never been molten and have the most refractory compositions. The second approach is sequential acid leaching of four CAIs from CV3 chondrites, including a fluffy Type A inclusion and one fine-grained inclusion, in order to chemically separate the various Ti-bearing phases in each individual CAI. This combined CAI Ti isotopic dataset is then used to infer the cause of Ti isotope heterogeneity in the CAI-forming region/process and the resulting implications for the composition of Ti-bearing solids in the solar parental molecular cloud.

Samples and Methods: Details regarding the CAIs investigated via LA-MC-ICPMS as well as the analytical procedures have been previously reported [5]. Four different types of CAIs (Table 1) were obtained for sequential acid leaching. A small fraction of each CAI powder was reserved for the bulk CAI Ti isotope measurement while the majority of each CAI powder was processed through a sequential acid leaching procedure modified from [6]. The CAI powders for the bulk measurements were digested on a hot plate using concentrated mineral acids. Chemical separation of Ti from the bulk CAIs and leachate samples followed previously established procedures [7-8]. All samples and standards were measured using the Neptune Plus MC-ICPMS in Münster, as outlined in [9]. To obtain Ti mass-independent (nucleosynthetic) data,

instrumental and natural mass fractionation were corrected using the exponential law and normalizing to ⁴⁹Ti/⁴⁷Ti = 0.749766.

Table 1– Characteristics of the CAIs for acid leaching.

CAI	Host meteorite	Mass for leaching (mg)	Mass for bulk Ti measurement (mg)	Description
Warrior	Acfer 082 (CV3)	92.5	15.8	FTA – FG
Pigeon	Acfer 082 (CV3)	50.3	4.6	CTA – FMG
Lizard	Allende (CV3.6)	22.8	8.2	A – FG
Garland	NWA 6619 (CV3)	7.4	3.5	C – CG

FTA = fluffy Type A, CTA = compact Type A, A = Type A, C = Type C, FG = fine-grained, FMG = fine- to medium-grained, CG = coarse-grained, NWA = Northwest Africa

Results and Discussion: The Ti isotopic data are reported utilizing the ϵ -notation (parts per ten thousand deviation from the standard). For the samples investigated via LA-MC-ICPMS (results shown in [5]), the majority of the $\epsilon^{50}\text{Ti}$ values are between 6-10, consistent with previously reported values for CAIs [*e.g.*, 8,10-14]. The coarse-grained CAIs define a range of $\epsilon^{50}\text{Ti}$ compositions from ~ -1 to 15 while the fine-grained and fluffy Type A CAIs span a larger range of $\epsilon^{50}\text{Ti}$ compositions from ~ -16 to 45. We also observe intra-CAI variation in $\epsilon^{50}\text{Ti}$ for some of the samples, although the widest variability is observed within the fine-grained and fluffy Type A CAIs.

The Ti isotope compositions of the four bulk CAIs and their six individual leachates are consistent with literature CAI Ti isotope data from ordinary, CM, CO, CV, and CK chondrites [*e.g.*, 8,10-14]. All four bulk CAIs and their leachates have small but resolvable excesses in $\epsilon^{48}\text{Ti}$ from the terrestrial composition ranging from 0.24 to 0.74. Garland, Pigeon, Lizard, and their corresponding leachates have excesses in $\epsilon^{46}\text{Ti}$ and $\epsilon^{50}\text{Ti}$ around 1.7 and 9.4, respectively (Fig. 1). In contrast, Warrior and its leachates are characterized by small deficits in $\epsilon^{46}\text{Ti}$ of ~ 0.2 and excesses in $\epsilon^{50}\text{Ti}$ of ~ 2 (Fig. 1).

The acid leachates from the two coarse-grained CAIs have little, if any, Ti isotope variability between the six different leaching steps for each individual CAI (Fig. 1). Given that these two CAIs were once molten, the homogenization of the Ti isotopes between the various Ti-bearing phases of the inclusions is expected. On the other hand, fine-grained CAIs did not experience melting and could potentially preserve vestiges of heterogeneous precursors. However, we observe that

the fine-grained inclusions also have little, if any, Ti isotope variability between the six different leaching steps. One clear difference between the two approaches utilized in this study is that the laser ablation data provides evidence of intra-CAI heterogeneity while the leachate data does not. The lack of variation in the Ti isotope compositions of the CAI acid leachates likely reflects that the leaching procedure is less effective in separating the different Ti-bearing phases compared to the laser technique.

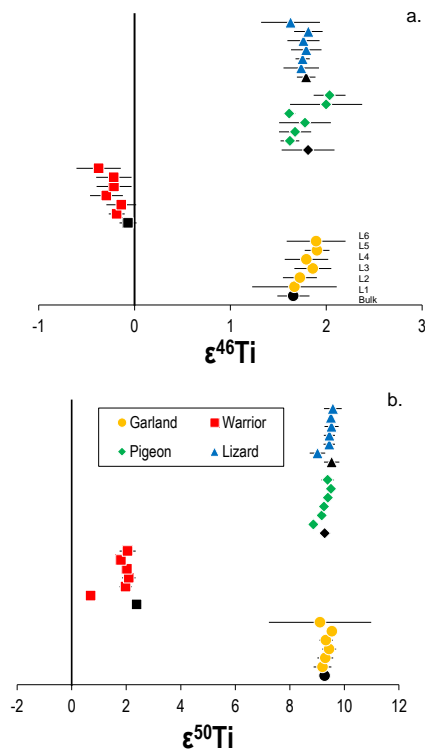


Fig. 1: The a) $\epsilon^{46}\text{Ti}$ and b) $\epsilon^{50}\text{Ti}$ data of the four CAIs and their corresponding leachates. Labeling for each sample is demonstrated by Garland.

The bulk CAIs and laser ablation spot analyses from this study as well as bulk CAI values from the literature all demonstrate heterogeneity in Ti isotopes in the CAI-forming region/process. This heterogeneity is shown in Fig. 2a with a normalized probability density plot for $\epsilon^{50}\text{Ti}$. Both the bulk CAI data and the laser ablation data comprise probability densities with a well-defined peak around $\epsilon^{50}\text{Ti}=9$. However, some CAI data fall outside of the main peak, indicating that there was heterogeneity in the precursor material from which the CAIs formed. We suggest that the variable Ti compositions amongst CAIs from CV, CK, CO, CM, and ordinary chondrites represents echoes of larger-scale heterogeneities in the precursor materials that have been dampened due to averaging.

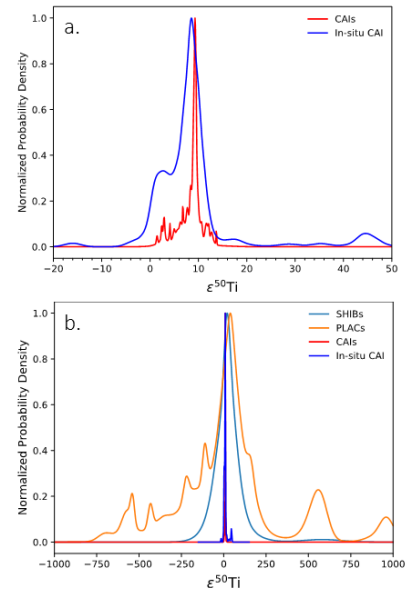


Fig. 2a/b: Normalized probability density plots for $\epsilon^{50}\text{Ti}$ showing a) normal CAIs and b) SHIBs, PLACs, and normal CAIs. Literature data compiled from [8, 12-19].

Hibonite-rich inclusions, including SHIBS and PLACs, have variable and large Ti isotope anomalies [e.g., 15-16], making hibonite grains attractive candidates for carriers of heterogeneous Ti isotope anomalies through to the CAI formation process. The coincidence of the peaks in probability distributions between SHIBs, PLACs, and CAIs suggests that the narrow distribution in CAIs compared with those for the hibonites in SHIBS and PLACs (Fig. 2b) is purely the result of averaging large numbers of smaller grains. Using typical sizes of hibonite grains ($30\ \mu\text{m}$) and CAIs ($600\ \mu\text{m}$), we find that the observed narrowing in the distributions from hibonites to CAIs is consistent with the prediction from the central limit theorem, suggesting that the heterogeneity in CAIs is an “echo” of the heterogeneity in hibonites. We propose that the heterogeneity in hibonites is in turn an echo of the much greater heterogeneity in the precursor presolar grains. Characterizing the dispersion in isotope anomalies at different scales of observation can be used to constrain models for mixing from the molecular cloud to the protoplanetary disk.

Acknowledgments: This work was funded by a Deutsche Forschungsgemeinschaft (DFG, German Research Foundation) research fellowship (project number 440227108). The authors thank I. Kohl for assistance with LA-MC-ICPMS.

References: [1] Dauphas & Schauble (2016) *Annu. Rev. Earth Planet. Sci.*, **44**, 709. [2] Burkhardt et al. (2019) *GCA*, **261**, 145. [3] Dauphas et al. (2010) *ApJ*, **720**, 1577. [4] Qin et al. (2011) *GCA*, **75**, 629. [5] Jordan et al. (2017) *LPSC*, **48**, #3032. [6] Reisberg et al. (2009) *EPSL*, **277**, 334. [7] Zhang et al. (2011) *J. Anal. At. Spectrom.*, **26**, 2197. [8] Torrano et al. (2019) *GCA*, **263**, 13. [9] Gerber et al. (2017) *ApJ*, **841**, L17. [10] Williams et al. (2016) *Chem. Geol.*, **436**, 1. [11] Simon et al. (2017) *EPSL*, **472**, 277. [12] Davis et al. (2018) *GCA*, **221**, 275. [13] Ebert et al. (2018) *EPSL*, **498**, 257. [14] Render et al. (2019) *GCA*, **254**, 40. [15] Kööp et al. (2016) *GCA*, **189**, 70. [16] Kööp et al. (2018) *EPSL*, **489**, 179. [17] Steele & Boehnke (2015) *ApJ*, **802**, 80. [18] Leya et al. (2009) *ApJ*, **702**, 1118. [19] Trinquier et al. (2009) *Science*, **324**, 374.